

See discussions, stats, and author profiles for this publication at: <https://www.researchgate.net/publication/231652330>

A New Class of Opacified Monolithic Aerogels of Ultralow High-Temperature Thermal Conductivities

ARTICLE *in* THE JOURNAL OF PHYSICAL CHEMISTRY C · APRIL 2009

Impact Factor: 4.77 · DOI: 10.1021/jp900380q

CITATIONS

19

READS

50

3 AUTHORS, INCLUDING:



Shih-Yuan Lu

National Tsing Hua University

159 PUBLICATIONS 3,080 CITATIONS

SEE PROFILE

A New Class of Opacified Monolithic Aerogels of Ultralow High-Temperature Thermal Conductivities

Te-Yu Wei,[†] Shih-Yuan Lu,^{*,‡} and Yu-Cheng Chang[‡]

Department of Chemical Engineering, National Tsing-Hua University, HsinChu, Taiwan 30013, Republic of China; Industrial Energy-Saving Technology Division, Energy & Environment Laboratories, Industrial Technology Research Institute, HsinChu, Taiwan 310, Republic of China

Received: January 14, 2009; Revised Manuscript Received: March 4, 2009

The development of materials of ultralow high-temperature thermal conductivities for applications in high-temperature thermal insulations has become increasingly more important than ever in view of the ever worsening issues of fossil energy depletion and global warming that call for more demanding energy-saving practices. In this study, a new class of opacified monolithic aerogels of ultralow high-temperature thermal conductivities was developed for thermal insulation applications at high temperatures. Carbon nanofibers were successfully incorporated into the mesoporous network of silica aerogels at concentrations as high as 20 wt % through an accelerated-gelation sol–gel process to enhance the dimensional stability of the silica aerogels and to suppress the thermal radiations that become dominant at high temperatures, to achieve an ultralow thermal conductivity of 0.050 W/m-K at 500 °C, whereas maintaining a thermal stability above 500 °C (much better than the conventional high-temperature thermal insulation materials: 0.3 W/m-K at 500 °C for glass fibers, 0.1 W/m-K at 527 °C for alumina fused brick, and 1.7 W/m-K at 527 °C for sillimante).

Introduction

The development of materials of ultralow high-temperature thermal conductivities for applications in high-temperature thermal insulations has become increasingly more important than ever in view of the ever worsening issues of fossil energy depletion and global warming that call for more demanding energy-saving practices. Silica aerogels, a class of mesoporous materials of extremely high porosities and specific surface areas, are an excellent candidate for thermal insulations because of the existence of a high percentage of highly interconnected pores.^{1–3} The apparent thermal conductivities of silica aerogels are commonly lower than 0.1 W/m-K at room temperature.^{1–3} Many industrial usages of thermal insulators, however, require application temperatures as high as 500 °C, at which point thermal radiations become dominant and greatly increase the thermal conductivities of the silica aerogels.^{4,5}

One promising way to improve the thermal insulation performance of silica aerogels at high temperatures up to 500 °C is to opacify the silica aerogels with materials of high specific extinction coefficients, particularly in the wavelength range of 3.75–5.06 μm , which corresponds to the temperature range of 500–300 °C. In addition to specific extinction coefficients, a good insulation material also needs to be thermally stable at high temperatures. Organic aerogels were once considered an alternative to silica aerogels as high temperature thermal insulation materials because of their high specific extinction coefficients, but they proved inappropriate because of their poor thermal stabilities at high temperatures.⁶ Carbon black and TiO₂ powders have been used as opacifiers for silica aerogels in recent years, but their

relatively large thermal conductivities, 4.18 and 6.5 W/m-K at room temperature, respectively, restrict their success.^{7–11} Although ultralow thermal conductivities of TiO₂-incorporated silica aerogels at high temperatures have been reported in the literature, such as that of 0.038 W/m-K at 527 °C reported in ref 8 and 0.0284 W/m-K at 400 °C reported in ref 11, these data were measured with the transient hot-wire method, and it is well-known that the transient hot-wire method is not suitable for thermal conductivity measurements of low bulk density materials such as silica aerogels, particularly at high temperatures, because of the serious thermal radiation disturbances, among other things.¹² In addition, carbon blacks are not thermally stable at temperatures above 300 °C.⁸ The quest for thermal insulation materials of ultralow high-temperature thermal conductivities continues.

In this work, carbon nanofibers (Yonyu, Taiwan) of low thermal conductivity (0.07 W/m-K at room temperature), high thermal stability (>500 °C), and high specific extinction coefficient in the wavelength range of 3.75–5.06 μm were incorporated into the mesoporous network of silica aerogels through an accelerated-gelation sol–gel process to achieve a thermal conductivity of 0.05 W/m-K at and a thermal stability above 500 °C. The thermal conductivity data were obtained with the hot-disk method (also called the transient plane source method), a new and accurate measurement method for thermal conductivity.¹³ The ultralow thermal conductivity of 0.05 W/m-K at 500 °C obtained in this work is much better than those of conventional high-temperature thermal insulation materials, such as glass fibers (0.3 W/m-K at 500 °C),¹⁴ alumina fused brick (0.1 W/m-K at 527 °C),⁸ and sillimante (1.7 W/m-K at 527 °C).⁸ Consequently, these carbon nanofiber incorporated composite silica aerogels should serve as excellent high-temperature thermal insulation materials and be useful for insulating boilers and buildings for energy-saving purposes.

* To whom correspondence should be addressed. E-mail: sylu@mx.nthu.edu.tw.

[†] National Tsing-Hua University.

[‡] Industrial Technology Research Institute.

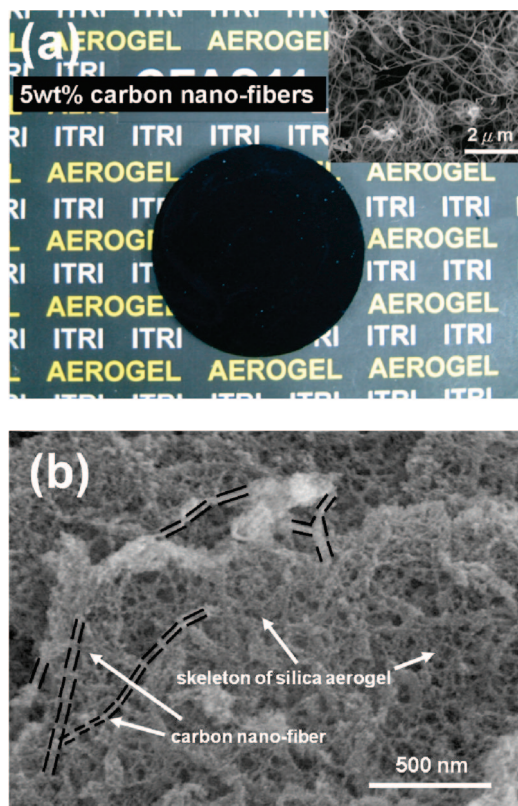


Figure 1. (a) Photograph of a monolith of a carbon nanofiber incorporated composite silica aerogel. The concentration of the carbon nanofiber was 5 wt %. The inset shows an SEM image of the carbon nanofibers. (b) An SEM image of a composite silica aerogel of 20 wt %, revealing the mesoporous structure and incorporated carbon nanofibers (guided with dashed lines).

Experiment

Synthesis of Carbon Nanofibers/SiO₂ Composite Aerogels.

The carbon nanofibers had diameters of 30–100 nm and lengths of up to 10 μm , as shown in the inset of Figure 1(a), and were added to the silica sol during a sol–gel process to afford the desired composite silica aerogel after supercritical drying with supercritical CO₂. We were able to incorporate as high as 20 wt % of carbon nanofibers into the silica aerogel before the fiber sedimentation issue became too serious to handle. In a typical run, tetraethoxysilane (20.8 g) was mixed with ethanol (13.8 g) and then HCl (1.8 g of 0.14 wt % HCl/H₂O solution) was added as the acidic catalyst for sol formation. The resulting mixture was stirred for 1.5 h, and then an ethanolic carbon nanofiber suspension of desired concentrations (carbon nanofiber suspension in 23 g of EtOH) was added to it. Some suitable

amount of 5 M NH₄OH (0.2 mL) was then added as the basic catalyst for gel formation. After 30 min of stirring, an excessive amount of 5 M NH₄OH (1.1 mL) was added to the mixture to further accelerate the gelation to avoid the sedimentation of carbon nanofibers.^{18–21} After 2 days of aging, the nonreacted chemicals were removed with ethanol, and this washing procedure was repeated every 24 h 3 times. The resulting wet gels were then dried with supercritical CO₂ to afford the composite silica aerogels.

Characterization of Composite Aerogels. The apparent density of the product was determined by dividing the product weight by the product volume. The porosity was calculated by $(1 - \rho_m/\rho_t) \times 100\%$. Here, ρ_m is the apparent density of the final product and ρ_t is the combined density of the silica and carbon nanofibers at a specified ratio. The Brunauer–Emmett–Teller (BET) specific surface area and Barrett–Joyner–Halenda (BJH) pore volume were obtained with the N₂ adsorption/desorption isotherms conducted at 77 K (Quantachrome, NOVA e1000). The morphology of the composite aerogel and carbon nanofibers were characterized with an FE-SEM (Hitachi-S4700). The thermal conductivities of the samples at desired temperatures were determined with the transient plane heat source method (Hot-Disk, Gothenburg, Sweden). The thermal stabilities of the composite aerogels and carbon nanofibers were characterized using thermogravimetry (TG) analysis from room temperature to 530 $^{\circ}\text{C}$ (Dupont Instruments, TGA951). The specific extinction coefficients of the samples were determined by FT-IR measurements (Perkin-Elmer Spectrum RX-I).

Result and Discussion

The product monoliths, all black and opaque, had diameters of 5.4–5.5 cm and thicknesses of 0.6–0.7 cm, as shown in Figure 1(a). Figure 1(b) shows an SEM image of the composite silica aerogel, revealing the mesoporous structure and incorporated carbon nanofibers. The relevant structural parameters and thermal conductivities are tabulated in Table 1. There are several points to be noted in Table 1. First, upon inclusion of the carbon nanofibers, the porosities of the silica aerogels were significantly increased, from 90.1% of the plain silica aerogel to 95.9% of the 0.5 wt % composite aerogel. This porosity jump may be attributed to the smaller extent of volume shrinkage during the supercritical drying procedure, effected by the enhanced dimensional stability by the incorporated carbon nanofibers. These carbon nanofibers served as a strong backbone for the composite, resisting volume shrinkage at the drying stage. The increase in porosity in turn leads to the decrease in room temperature thermal conductivity of the silica aerogel, from 0.041 of the plain silica aerogel to 0.0295 W/m-K of the 0.5 wt % composite

TABLE 1: Structural Properties and Thermal Conductivities of Composite Silica-Carbon Fiber Aerogels

	density ^c (g/cm ³)	porosity (%)	BET surface area (m ² /g) ^d	BJH pore volume (cm ³ /g) ^e	thermal conductivity (W/m-K) ^f
aerogel ^a	0.218 \pm 0.002	90.1	1199	3.43	0.0410 \pm 0.0003
0.5 wt % ^b	0.090 \pm 0.004	95.9	848	5.23	0.0295 \pm 0.0026
1 wt % ^b	0.095 \pm 0.003	95.7	844	4.92	0.0316 \pm 0.0010
5 wt % ^b	0.097 \pm 0.003	95.5	830	5.02	0.0329 \pm 0.0006
10 wt % ^b	0.109 \pm 0.003	95.0	829	4.80	0.0334 \pm 0.0003
13 wt % ^b	0.111 \pm 0.002	94.9	765	4.77	0.0352 \pm 0.0003
15 wt % ^b	0.111 \pm 0.006	94.8	746	4.44	0.0370 \pm 0.0006
20 wt % ^b	0.110 \pm 0.005	94.8	696	4.43	0.0380 \pm 0.0023

^a Plain silica aerogels. ^b Weight percentage of carbon nanofibers. ^c Average of six samples. ^d BET specific surface area obtained with the BET model at P/P_0 from 0.1 to 0.3. ^e BJH pore volume obtained with the BJH model from N₂ desorption data. ^f Thermal conductivity at room temperature.

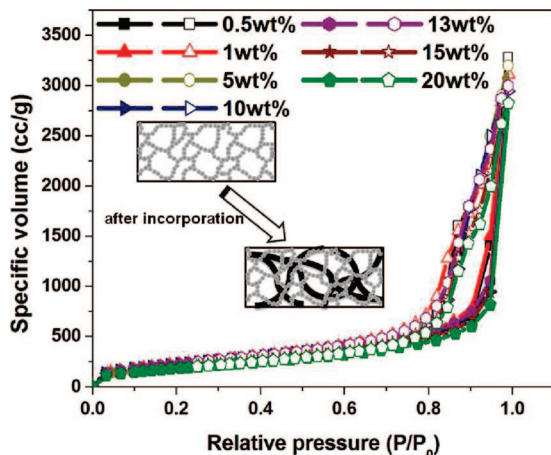


Figure 2. N_2 adsorption/desorption isotherms (at 77 K) of seven composite silica aerogels of increasing carbon nanofiber loadings: 0.5, 1, 5, 10, 13, 15, and 20 wt %. The inset shows an illustration of the incorporation of the carbon nanofibers.

aerogel. The higher porosity, the less thermally more conducting solid content in the composite, generally leads to lower overall thermal conductivities. The porosity, however, dropped slightly with an increasing amount of the carbon nanofiber, probably because of the increasing occupancy of the pore volume by the carbon nanofibers, as illustrated in the inset of Figure 2. As a result, the pore volume decreased from 5.23 to 4.43 cm^3/g , and room temperature thermal conductivities increased slightly from 0.0295 to 0.0380 W/m·K with the nanofiber loading increasing from 0.5 to 20 wt %. The increasing occupancy of the carbon nanofibers in the pore space also resulted in a significant decrease in the specific surface area, since the diameter of the nanofiber (30–100 nm) is larger than that of the primary particle diameter of the silica backbone (<10 nm).^{1–3}

The structural parameters, including porosity, specific surface area, and pore volume, of the samples were derived from the N_2 adsorption/desorption isotherms of the samples at 77 K. The specific surface area data were based on the BET model, whereas the pore structure parameters were derived from the BJH model. As shown in Figure 2, all samples exhibited type IV isotherms with a type H3 hysteresis loop, typical for mesoporous materials such as silica aerogels.¹⁵ The limited N_2 uptake obtained at low relative pressures (<0.1) indicated the existence of a mesoporous structure in which capillary condensation occurred, limiting the growth in N_2 uptake.¹⁶ Evidently, the inclusion of the carbon nanofibers did not alter the basic mesoporous nature of the aerogels, although significant changes in structural parameters such as porosity, specific surface area, and pore volume did occur.

The thermal conductivities of the samples of increasing nanofiber loading, determined with the hot-disk method (Göteborg, Sweden)^{13,21} as a function of temperature are shown in the inset of Figure 3(a). As expected, the thermal conductivities of the samples increased with increasing temperature. One of the main contributors to this increasing trend is the intensified thermal radiations at high temperatures. In addition, the mesoporous structure of the sample further densifies at high temperatures, leading to lower porosities and, thus, higher thermal conductivities. The increasing trend in thermal conductivity with respect to temperature was most pronounced for the plain silica aerogel case and was significantly moderated for the composite silica aerogel cases. For plain silica aerogels, the thermal conductivity increase ratio at 500 °C, defined as $(k_{500} - k_{RT})/k_{RT}$, was 1.31 (k_{RT} denotes the thermal conductivity at room

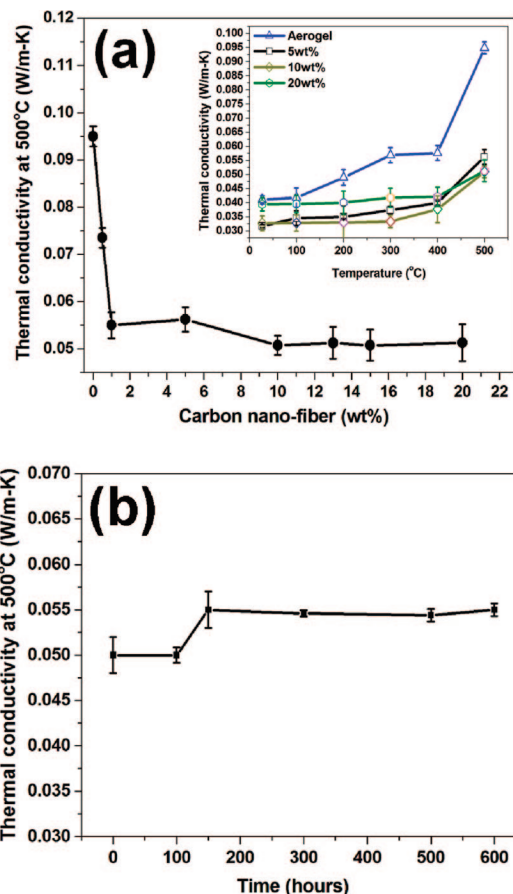


Figure 3. (a) Thermal conductivities of composite silica aerogels at 500 °C as a function of the carbon nanofibers loading. The inset shows the thermal conductivity versus temperature curves for the composite silica aerogels of increasing carbon nanofiber loading: 0, 5, 10, 20 wt %. (b) Thermal stability of a composite silica aerogel of 10 wt % in terms of the thermal conductivity at 500 °C, tested for a long time period of 25 days.

temperature), much larger than that of 0.30 for the composite silica aerogels of 20 wt %. In fact, this ratio decreased with increasing nanofiber loading, indicating the effective suppression of thermal radiations by the incorporated carbon nanofibers. Table 2 shows the decreasing trend of this ratio with increasing nanofiber loading. One may wonder why the increase ratio for the 0.5 wt % composite aerogel, 1.33, is larger than that of the plain silica aerogel. For the case of the 0.5 wt % composite aerogel, its k_{RT} dropped significantly because of the much improved porosity, whereas its k_{500} was not improved as much due to the limited amount of nanofiber inclusion for thermal radiation suppression. Note also the comparison in data of 1 and 5 wt % did not follow the decreasing trend. This discrepancy was probably caused by the possible measurement errors involved in the k_{500} values of 1 and 5 wt %.

Figure 3(a) shows the thermal conductivities at 500 °C as a function of the carbon nanofiber loading. Evidently, the values of k_{500} decreased sharply with increasing carbon nanofiber loading and started leveling off at a carbon nanofiber loading of about 10 wt %. Figure 3(b) shows the long-term thermal stability of the composite silica aerogels in terms of the thermal conductivity, by holding the samples at 500 °C for a time period of 600 h (25 days). The jump in thermal conductivity that occurred in the time period of 100–150 h may be caused by additional volume shrinkage of the samples and continuing condensation of the hydroxide groups of the silica backbone after a long time holding at high temperatures. The values of

TABLE 2: The Thermal Conductivity Increase Ratio at 500 °C, Defined as $(k_{500} - k_{RT})/k_{RT}$, of the Plain and Composite Silica Aerogels at an Increasing Loading of Carbon Nanofibers

		wt %						
	aerogel	0.5	1	5	10	13	15	20
$(k_{500} - k_{RT})/k_{RT}$	1.31	1.33	0.74	0.75	0.56	0.45	0.37	0.30

k_{500} , however, remained almost constant (0.055 W/m-K) after the jump, indicating an excellent thermal stability of the composite silica aerogels at 500 °C.

The thermal stability of the composite silica aerogels was further characterized by the thermogravimetry analysis. Figure 4 shows the weight loss-vs-time curves for a plain silica aerogel and a composite silica aerogel of 10 wt %. The samples were heated to 530 °C from room temperature with a heating rate of 10 °C/min and held at 530 °C afterward. There can be observed two weight loss stages. The first weight loss stage was steep and was caused by the removal of the adsorbed water. Note here the present products, plain or composite silica aerogels, were hydrophilic and can adsorb a large amount of water when placed in ambient atmosphere. In the second weight loss stage, the hydroxide groups distributed on the surfaces of the silica backbone were removed through condensation at higher temperatures.¹⁷ The weight loss curves then slowly leveled off after the second weight loss stage, indicating the good thermal stability of the samples at 530 °C. If the temperature was further increased to 600 °C, the carbon nanofibers were thermally decomposed, and the originally black composite silica aerogel turned transparent, as shown in the inset of Figure 4. The porosity of this transparent silica aerogel was slightly increased by an amount of 0.21 %, as compared with the starting 10 wt % composite aerogel. This is a result of two competing effects: one is the removal of the nanofibers to increase the porosity and the other is the intensified volume shrinkage at the heat treatment for loss of the nanofibers, the structural stabilizer, to decrease the porosity. This slight increase in porosity led to a slight decrease in room temperature thermal conductivity to 0.0330 W/m-K, 1.2% lower than that of the starting 10 wt % composite aerogel.

The ultralow high-temperature thermal conductivities of the composite aerogels were attributed to the incorporation of the

carbon nanofibers. These carbon nanofibers, in addition to offering enhanced dimensional stability, possessed high specific extinction coefficients in the wavelength range of 3.75–5.06 μm , equivalent to the temperatures range of 500–300 °C, and significantly suppressed the thermal radiation contributions to the thermal conductivities at temperatures up to 500 °C. Here, we investigate the specific extinction coefficients of the products to support our arguments. The specific extinction coefficient was determined on the basis of the Fourier transform infrared (FTIR) spectroscopy of the samples.⁴ Samples (0.004 g) were ground into powders and then pressed to form disks of a thickness of 0.15 mm and a diameter of 12.6 mm. The specific extinction coefficient was computed on the basis of the Beer–Lambert law:

$$\alpha = A \times 2.303/CL \quad (1)$$

Here, α , A , C , and L are the specific extinction coefficient, absorption intensity of FTIR, sample concentration (mass/volume), and distance of the light traveling through the sample, respectively. Figure 5 shows the specific extinction coefficients of four samples, including a plain silica aerogel and three composite silica aerogels of 0.5, 10, and 20 wt % in the wavelength range of 3–9 μm . Evidently, the plain silica aerogel possessed a high specific extinction coefficient in the wavelength range longer than 8 μm , corresponding to temperatures lower than 100 °C. These high specific extinction coefficients, however, do not help to suppress thermal radiations emitted at temperatures higher than 100 °C.⁴ In the wavelength range of 3.5–7 μm , the specific extinction coefficients increased with increasing loading of the carbon nanofibers. Of particular importance are the much improved specific extinction coefficients in the wavelength range of 3.75–5.06 μm , corresponding to thermal radiations of 500–300 °C and highlighted in Figure 5 with a rectangle, achieved with the incorporation of the carbon nanofibers. For the case of 0.5 wt %, the limited amount of nanofiber incorporation restricted the improvement in specific

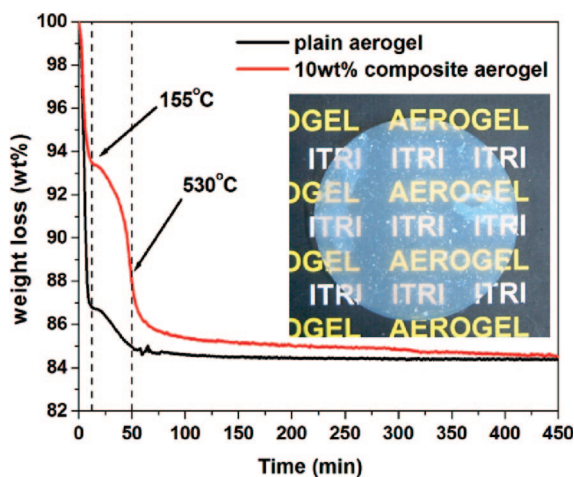


Figure 4. Thermogravimetry analysis curves of a plain silica aerogel and a composite silica aerogel of 10 wt %. The temperature was increased from room temperature to 530 °C with a heating rate of 10 °C/min and held at 530 °C afterward. The inset shows a photograph of a composite silica aerogel of 10 wt % after the thermal treatment at 600 °C.

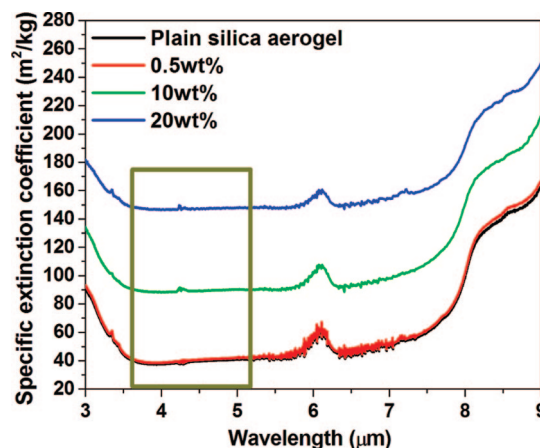


Figure 5. Specific extinction coefficient-vs-wavelength curves for a plain silica aerogel and three composite silica aerogels of 0.5, 10, and 20 wt %.

extinction coefficient. The improvement in k_{500} of this case, as shown in Figure 3(a), was mainly contributed by the low k_{RT} achieved with the porosity increase. At high enough nanofiber loadings, the resulting high specific extinction coefficients gave rise to much suppressed thermal radiations at temperatures higher than 300 °C, leading to the ultralow thermal conductivities at 500 °C. Note that the thermal conductivity increase ratio at 500 °C decreased from 0.74 to 0.3 with the nanofiber loading increasing from 1 to 20 wt %. The effect of the thermal radiation suppression, however, reached its saturation at about 10 wt % of the nanofiber inclusion, leading to a leveling off of k_{500} .

In conclusion, an accelerated-gelation sol–gel process was developed to incorporate carbon nanofibers of up to 20 wt % to the mesoporous structure of silica aerogels. The high specific extinction coefficients of these carbon nanofibers in the wavelength range of 3.75–5.06 μm effectively suppressed the intensified thermal radiations at high temperatures to achieve ultralow thermal conductivities at 500 °C. Long-term thermal stability of such composite silica aerogels was demonstrated, implying the suitability of the present products to serve as high-temperature thermal insulation materials.

Acknowledgment. The authors gratefully acknowledge the financial support of the Bureau of Energy, Ministry of Economic Affairs, Taiwan, Republic of China and the assistance offered by ITRI, Taiwan, Republic of China for the thermal conductivity measurements.

References and Notes

- (1) Kistler, S. S. *Nature (London)* **1931**, 227, 741.
- (2) Hüsing, N.; Schubert, U. *Angew. Chem., Int. Ed.* **1998**, 37, 22.
- (3) Pierre, A. C.; Pajonk, G. M. *Chem. Rev.* **2002**, 102, 4243.
- (4) Frick, J. *Proc. Phys.* **6** **1985**, 100.
- (5) Schwertfeger, F.; Schubert, U. *Chem. Mater.* **1995**, 7, 1909.
- (6) Lu, X.; Arduini-Schuster, M. C.; Kuhn, J.; Nilsson, O.; Frick, J.; Pekala, R. W. *Science* **1992**, 255, 971.
- (7) Hrubesh, L. W.; Pekala, R. W. *J. Mater. Res.* **1994**, 9, 731.
- (8) Wang, J.; Kuhn, J.; Lu, X. *J. Non-Cryst. Solids* **1995**, 186, 296.
- (9) Kuhn, J.; Gleissner, T.; Arduini-Schuster, M. C.; Korder, S.; Frick, J. *J. Non-Cryst. Solids* **1995**, 186, 291.
- (10) Zeng, S. Q.; Hunt, A.; Greif, R. *J. Non-Cryst. Solids* **1995**, 186, 271.
- (11) Kwon, Y. G.; Choi, S. Y.; Kang, E. S.; Baek, S. S. *J. Mater. Sci.* **2000**, 35, 6075.
- (12) Wulf, R.; Barth, G.; Gross, U. *Int. J. Thermophys.* **2007**, 28, 1679.
- (13) Al-Ajlani, S. A. *Appl. Thermal Eng.* **2006**, 26, 2184.
- (14) www.osti.gov/bridge/product.biblio.jsp?query_id=0&page=0&osti_id=885664 (March, 2009).
- (15) Jeong, A. Y.; Koo, S. M.; Kim, D. P. *J. Sol-Gel Sci. Technol.* **2000**, 19, 483.
- (16) Sing, K. S. W. *Pure Appl. Chem.* **1982**, 54, 2201.
- (17) Brinker, C. J.; Scherer, G. W. *Sol-Gel Sci.* **1990**, 557.
- (18) Wei, T. Y.; Chang, T. F.; Lu, S. Y.; Chang, Y. C. *J. Am. Ceram. Soc.* **2007**, 90, 2003.
- (19) Wei, T. Y.; Lu, S. Y.; Chang, Y. C. *J. Chin. Inst. Chem. Eng.* **2007**, 38, 477.
- (20) Wei, T. Y.; Kuo, C. Y.; Hsu, Y. J.; Lu, S. Y.; Chang, Y. C. *Microporous Mesoporous Mater.* **2008**, 112, 580.
- (21) Wei, T. Y.; Lu, S. Y.; Chang, Y. C. *J. Phys. Chem. B* **2008**, 112, 11881.

JP900380Q